

homogeneous soil with an impervious barrier. The numerical solution requires a very long computational time and a large storage capacity of the computer; in addition the problems of stability and convergence should be considered. Moreover the Gauss principle of least constraint was used as an appropriate direct method for solving the linear and non-linear heat conduction problems [6].

The objective of the present study is to apply the Gauss principle of least constraint to the infiltration from semi-circular furrows and buried pipes into unsaturated soils and to compare the results with those obtained by the ADI method.

GAUSS PRINCIPLE

Gauss principle of least constraint is a true minimum principle applied in classical mechanics. It could be used to treat the non-linear diffusion equation which governs the two-dimensional flow of water in unsaturated soils

$$\frac{\partial(\theta)}{\partial t} = \text{div} (D(\theta) \text{ grad } \theta) - \frac{\partial k(\theta)}{\partial z} \quad \dots\dots\dots(1)'$$

where; θ is the volumetric moisture content (cm^3/cm^3),
 $D(\theta)$ is the soil water diffusivity (cm^2/min),
 $k(\theta)$ is the capillary conductivity (cm/min),
 t is the time,

Equation (1)' could be rewritten as

$$\frac{\partial \theta}{\partial t} - \frac{\partial}{\partial x} \left(D(\theta) \frac{\partial \theta}{\partial x} \right) + \frac{\partial}{\partial z} \left(D(\theta) \frac{\partial \theta}{\partial z} \right) - \frac{\partial k(\theta)}{\partial z} = 0 \quad \dots(1)$$

where; x is the horizontal coordinate (cm),
 z is the vertical coordinate (positive downwards), (cm).

The diffusion analog of Gauss principle expression (6) can be written as follows:

$$G = \int_v [P - Q]^2 dv, \quad (2)$$

where v is the volume engaged in the process of diffusion,
 $P = \partial\theta/\partial t$,
 $Q = \text{div}(D(\theta) \text{ grad } \theta) - \partial k(\theta)/\partial z$;
 P and Q are the temporal and spatial parts respectively.

Let us seek a solution of equation (1) which belongs to a family of functions with one or more unknown parameters. In each particular case the characteristic complex of the parameters, which represents P or Q must be identified and a minimization of the constraint G has to be performed with respect to one of these complexes. So the problem reduces to the algebraic minimization of a polynomial with respect to some complex of physical parameters.

In the following study the Gauss principle is applied to the infiltration from semi-circular furrows and from buried pipes.

1. THE INFILTRATION FROM EQUALLY SPACED SEMI-CIRCULAR FURROWS

Figure (1) shows the flow medium which is a homogeneous soil underlain by a horizontal impervious barrier at some depth Z from the soil surface. The water source is a set of semi-circular furrows of radius R spaced at regular intervals $2X$. Due to the symmetry of the system, the soil medium can be divided into rectangular slabs and confine the solution to one single slab, e.g. ABCDE, since there is no flow from one slab to the other. The origin of the rectangular system of coordinates x and z is placed at the centre of the furrow.

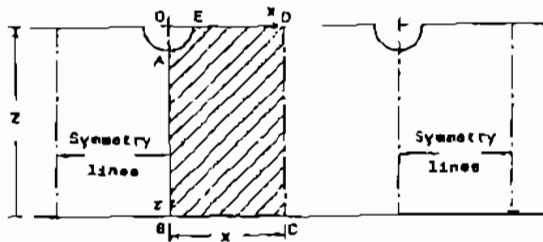


Fig.(1) Schematic diagram of a homogeneous soil irrigated by a set of semi-circular furrows equally spaced at distances of $2X$.

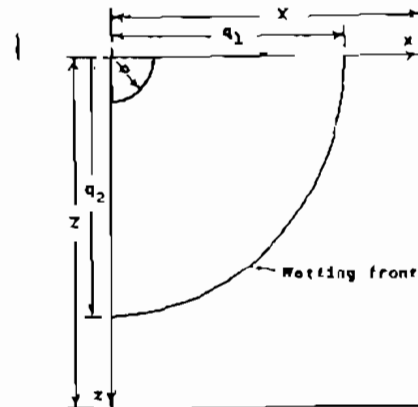


Fig.(2) Schematic diagram of the wetting front in the case of the furrow.

A constant low water content θ_1 throughout the flow medium is considered as the initial condition:

$$\theta = \theta_1, \quad x^2 + z^2 > R^2, \quad \left| \begin{array}{l} 0 \leq x \leq X \\ 0 \leq z \leq Z \end{array} \right|, \quad t = 0. \quad (3)$$

The boundary conditions are:

- 1- Along the furrow surface AE , the water content is always maintained at saturation θ_s :

$$\theta = \theta_s \quad \text{for} \quad x^2 + z^2 = R^2, \quad t \geq 0. \quad (4)$$

- 2- There is no horizontal flow across the vertical lines of symmetry AB and CD :

$$\frac{\partial \theta}{\partial x} = 0 \quad \text{for} \quad \left| \begin{array}{l} x = 0 \quad R \leq z \leq Z \\ x = X \quad 0 \leq z \leq Z \end{array} \right|, \quad t \geq 0. \quad (5)$$

- 3- There is no vertical flow across the soil surface ED and the

Impervious barrier BC:

$$- D(\theta) \frac{\partial \theta}{\partial z} + k(\theta) = 0 \quad \text{for} \quad \left| \begin{array}{l} z = 0, \quad R \leq x \leq X \\ z = 2, \quad 0 \leq x \leq X \end{array} \right|, \quad t \geq 0. \quad (6)$$

METHOD OF SOLUTION

To obtain an approximate trial solution, the capillary term in equation (1) is neglected so that the resulting equation, in polar coordinates, becomes

$$\frac{\partial \theta}{\partial t} = \frac{1}{r} \frac{\partial}{\partial r} \left(r D(\theta) \frac{\partial \theta}{\partial r} \right). \quad (7)$$

Using Boltzmann transformation $\phi = r t^{-1/2}$, then equation (7) can be reduced to the ordinary differential equation

$$- \frac{\phi}{2} \frac{d\theta}{d\phi} = \frac{1}{\phi} \frac{d}{d\phi} \left(\phi D(\theta) \frac{d\theta}{d\phi} \right). \quad (8)$$

Regarding experimental results the general form of $D(\theta)$ is found to be (5)

$$D(\theta) = A_1 e^{A_2 \theta}, \quad (9)$$

where A_1 and A_2 are known constants.

Substituting equation (8) into equation (9) and neglecting the terms of less weight, then

$$- \frac{\phi}{2} = A_1 A_2 e^{A_2 \theta} \left(\frac{d\theta}{d\phi} \right). \quad (10)$$

The integration of this equation gives

$$\theta = \frac{1}{A_2} \ln \left[\frac{C}{A_1} - \frac{\phi^2}{4A_1} \right], \quad (11)$$

where C is the integration constant.

Equation (11) shows that the advance of the wetting front is the same in both directions due to the drop of the gravity influence. Actually different advances should occur in both directions so that the trial function (11) may be modified to have the form

$$\theta = C_0 + C_1 \ln \left[1 - C_2 \left(\frac{x^2}{q_1^2} + \frac{z^2}{q_2^2} \right) \right], \quad (12)$$

where the constants C_0 , C_1 and C_2 and the functions of time q_1 and q_2 are unknowns to be determined. The functions q_1 and q_2 represent the penetration depths of the wetting front in the horizontal and

vertical directions respectively, Figure (2).

The trial function (12) fails to satisfy the boundary conditions (4) and (6) so that some modifications are necessary. Nevertheless a variation of the trial function results in very complicated integrals. Hence, the boundary conditions should be approximated to suit the trial function. The boundary conditions can be approximated as follows :

$$1- \theta = \theta_B ; \quad x = z = 0 ; \quad t \geq 0 ; \\ q_1 = q_2 = R ; \quad t = 0. \quad (13)$$

$$2- (\partial\theta/\partial x) = 0 ; \quad x = 0 ; \quad R < z < q_2 . \quad (14)$$

$$3- (\partial\theta/\partial z) = 0 ; \quad z = 0 ; \quad R \leq x \leq q_1 . \quad (15)$$

$$4- \theta = \theta_w ; \quad \frac{x^2}{q_1^2} + \frac{z^2}{q_2^2} = 1 . \quad (16)$$

The substitution of the boundary condition (13) in the trial function (12) gives $C_0 = \theta_B$. Hence the trial function becomes

$$\theta = \theta_B + C_1 \ln \left(1 - C_2 \left(\frac{x^2}{q_1^2} + \frac{z^2}{q_2^2} \right) \right) \quad (17)$$

Using the trial function (17), the integral of the right-hand side of equation (2) can be evaluated knowing that the general form of $k(\theta)$ is [5]

$$k(\theta) = A_3 e^{A_4 \theta - A_5 \theta^2} ,$$

where A_3 , A_4 and A_5 are known constants.

From the partial derivative $(\partial\theta/\partial t)$, the temporal complex

$$w_1 = \dot{q}_1/q_1 \quad \text{and} \quad w_2 = \dot{q}_2/q_2. \quad (18)$$

is determined, while the spatial complex can be obtained from the terms

$$\frac{\partial}{\partial x} \left(D(\theta) \frac{\partial \theta}{\partial x} \right), \quad \frac{\partial}{\partial z} \left(D(\theta) \frac{\partial \theta}{\partial z} \right) \quad \text{and} \quad \frac{\partial k(\theta)}{\partial z}, \quad \text{namely,}$$

$$k_1 = \frac{1}{q_1^2} \quad \text{and} \quad k_2 = \frac{1}{q_2^2} . \quad (19)$$

Using equations (18) and (19) equation (2) becomes

$$G = B_1 q_1 q_2 [3w_1^2 + 2w_1 w_2 + 3w_2^2] + q_1 q_2 (3B_2 - B_3 + B_4) [k_1^2 + k_2^2] \\ + B_5 q_1 q_2 k_2 - B_6 q_1 q_2 (w_1(3k_1 + k_2) + w_2(k_1 + 3k_2)) \\ + B_7 q_1 q_2 (w_1 + w_2)(k_1 + k_2) + B_8 q_1 (w_1 + 2w_2) \\ + 2(B_2 - B_3 + B_4) q_1 q_2 k_1 k_2 - (B_9 - B_{10}) q_1 k_1 - (2B_9 - B_{10}) q_1 k_2, \quad (20)$$

where :

$$B_1 = \frac{\pi}{4} C_1^2 C_2 \left(\frac{1}{C_2} + \frac{1}{2(1-C_2)} + \frac{\ln(1-C_2)}{C_2^2} \right) \quad (21)$$

$$B_2 = \pi A_2^2 C_1^2 C_2^3 (A_2 C_1 - 1)^2 e^{2A_2 \theta_S} \cdot \left[\frac{1 - (1 - C_2)^{2A_2 C_1 - 1}}{C_2^2 (2A_2 C_1 - 1)(2A_2 C_1 - 2)(2A_2 C_1 - 3)} - \frac{(1 - C_2)^{2A_2 C_1 - 2}}{C_2(2A_2 C_1 - 2)(2A_2 C_1 - 3)} - \frac{(1 - C_2)^{2A_2 C_1 - 3}}{2(2A_2 C_1 - 3)} \right] \quad (22)$$

$$B_3 = 2\pi A_1^2 C_1^2 C_2^2 (A_2 C_1 - 1) e^{2A_2 \theta_S} \left[\frac{1 - (1 - C_2)^{2A_2 C_1 - 1}}{C_2(2A_2 C_1 - 1)(2A_2 C_1 - 2)} - \frac{(1 - C_2)^{2A_2 C_1 - 2}}{(2A_2 C_1 - 2)} \right] \quad (23)$$

$$B_4 = \pi A_1^2 C_1^2 C_2 e^{2A_2 \theta_S} \left(\frac{1 - (1 - C_2)^{2A_2 C_1 - 1}}{2A_2 C_1 - 1} \right) \quad (24)$$

$$B_5 = \pi A_3^2 C_1^2 C_2^2 e^{2\theta_S(A_4 - A_5 \theta_S)} \cdot \int_0^1 a^3 \left[-A_4 + 2A_5(\theta_S + C_1 \ln(1 - C_2 a^2)) \right]^2 \cdot [1 - C_2 a^2]^{2C_1(A_4 - A_5(2\theta_S + C_1 \ln(1 - C_2 a^2)))} - 2 da \quad (25)$$

$$B_6 = \pi A_1 C_1^2 C_2^2 (A_2 C_1 - 1) e^{A_2 \theta_S} \left[\frac{1 - (1 - C_2)^{A_2 C_1}}{C_2^2 (A_2 C_1)(A_2 C_1 - 1)(A_2 C_1 - 2)} - \frac{(1 - C_2)^{A_2 C_1 - 1}}{C_2(A_2 C_1 - 1)(A_2 C_1 - 2)} - \frac{(1 - C_2)^{A_2 C_1 - 2}}{2(A_2 C_1 - 2)} \right] \quad (26)$$

$$B_7 = \kappa A_1 C_1^2 C_2 e^{A_2 \theta_S} \left[\frac{1 - (1 - C_2)^{A_2 C_1}}{C_2 (A_2 C_1) (A_2 C_1 - 1)} - \frac{(1 - C_2)^{A_2 C_1 - 1}}{(A_2 C_1 - 1)} \right] \quad (27)$$

$$B_8 = \frac{8}{3} A_3 C_1^2 C_2^2 e^{\theta_S (A_4 - A_5 \theta_S)} \cdot \int_0^1 a^4 \{-A_4 + 2A_5(\theta_S + C_1 \ln(1 - C_2 a^2))\} \cdot (1 - C_2 a^2)^{C_1 (A_4 - A_5 (2\theta_S + C_1 \ln(1 - C_2 a^2))) - 2} da \quad (28)$$

$$B_9 = \frac{16}{3} A_1 A_3 C_1^2 C_2^3 (A_2 C_1 - 1) e^{\theta_S (A_2 + A_4 - A_5 \theta_S)} \cdot \int_0^1 a^4 \{-A_4 + 2A_5(\theta_S + C_1 \ln(1 - C_2 a^2))\} \cdot (1 - C_2 a^2)^{C_1 (A_2 + A_4 - A_5 (2\theta_S + C_1 \ln(1 - C_2 a^2))) - 3} da \quad (29)$$

$$B_{10} = 8 A_1 A_3 C_1^2 C_2^2 e^{\theta_S (A_2 + A_4 - A_5 \theta_S)} \cdot \int_0^1 a^2 \{-A_4 + 2A_5(\theta_S + C_1 \ln(1 - C_2 a^2))\} \cdot (1 - C_2 a^2)^{C_1 (A_2 + A_4 - A_5 (2\theta_S + C_1 \ln(1 - C_2 a^2))) - 2} da \quad (30)$$

MINIMIZATION WITH RESPECT TO THE TEMPORAL COMPLEX

Minimization of the constraint (20) with respect to the temporal complex w_1 and w_2 implies that

$$(\partial G / \partial w_1) = B_1 q_1 q_2 (6w_1 + 2w_2) - B_6 q_1 q_2 (3k_1 + k_2) + B_7 q_1 q_2 (k_1 + k_2) + B_8 q_1 = 0 \quad (31)$$

and

$$(\partial G / \partial w_2) = B_1 q_1 q_2 (2w_1 + 6w_2) - B_6 q_1 q_2 (k_1 + 3k_2) + B_7 q_1 q_2 (k_1 + k_2) + 2B_8 q_1 = 0 \quad (32)$$

Solving equations (31) and (32) for w_1 and w_2 and substituting from (18) and (19) we have:

$$\begin{aligned} \dot{q}_1 &= \frac{4B_6 - B_7}{8B_1} \frac{1}{q_1} - \frac{B_7}{8B_1} \frac{q_1}{q_2^2} - \frac{B_8}{16B_1} \frac{q_1}{q_2}, \\ \dot{q}_2 &= \frac{4B_6 - B_7}{8B_1} \frac{1}{q_2} - \frac{B_7}{8B_1} \frac{q_2}{q_1^2} - \frac{5B_8}{16B_1}. \end{aligned} \quad (33)$$

MINIMIZATION WITH RESPECT TO THE SPATIAL COMPLEX

The minimization of constraint (20) with respect to the spatial complex k_1 and k_2 gives

$$\begin{aligned} \dot{q}_1 &= \frac{B_6(4B_2 - B_3 + B_4) - B_2 B_7}{B_6(2B_6 - B_7)} \frac{1}{q_1} - \frac{B_6(B_3 - B_4) - B_2 B_7}{B_6(2B_6 - B_7)} \frac{q_1}{q_2^2} \\ &\quad - \frac{1}{4} \frac{B_6(B_9 - 2B_{10}) + B_7 B_9}{B_6(2B_6 - B_7)} \frac{q_1}{q_2} - \frac{1}{4} \frac{B_5(B_6 - B_7)}{B_6(2B_6 - B_7)} \frac{q_1}{q_1}, \\ \dot{q}_2 &= \frac{B_6(4B_2 - B_3 + B_4) - B_2 B_7}{B_6(2B_6 - B_7)} \frac{1}{q_2} - \frac{B_6(B_3 - B_4) - B_2 B_7}{B_6(2B_6 - B_7)} \frac{q_2}{q_1^2} \\ &\quad - \frac{1}{4} \frac{B_6(5B_9 - 2B_{10}) - B_7 B_9}{B_6(2B_6 - B_7)} + \frac{1}{4} \frac{B_5(3B_6 - B_7)}{B_6(2B_6 - B_7)} \frac{q_2}{q_2}. \end{aligned} \quad (34)$$

The solution of the coupled systems of differential equations (33) or (34) gives the value of the penetration depths q_1 and q_2 as functions of time. It should be noted that the coefficients in the differential equations depend on the values of the constants C_1 and C_2 .

CALCULATION OF THE CONSTANTS

For simplicity the effect of gravity can be neglected, hence equation (17) becomes

$$\theta = \theta_s + C_1 \ln(1 - C_2 (r^2/q^2)), \quad (35)$$

where $r^2 = x^2 + z^2$.

The condition to be satisfied at the wetting front is

$$-D(\theta) \left(\frac{\partial \theta}{\partial r} \right) \Big|_{\theta = \theta_v} = (\theta_w - \theta_1) \dot{q}.$$

Substituting from equation (35), then

$$\dot{q} = \frac{D(\theta_w)}{\theta_w - \theta_1} \frac{2 C_1 C_2}{1 - C_2} \frac{1}{q}. \quad (36)$$

Also, if the influence of gravity is ignored, the coupled systems of differential equations (33) and (34) become respectively :

$$\dot{q} = \frac{2B_6 - B_7}{4B_1} \frac{1}{q}, \quad (37)$$

$$\dot{q} = \frac{2B_2 - B_3 + B_4}{2B_6 - B_7} \frac{1}{q}. \quad (38)$$

Comparison of the coefficients of equations (36) and (37) gives

$$8D(\theta_v) C_1 C_2 B_1 = (\theta_v - \theta_1)(1 - C_2)(2B_6 - B_7), \quad (39)$$

while that of equations (36) and (38) gives

$$D(\theta_v) C_1 C_2 (2B_6 - B_7) - (\theta_v - \theta_1)(1 - C_2)(2B_2 - B_3 + B_4) = 0. \quad (40)$$

The substitution of the condition (16) in the trial function (17) yields

$$C_2 = 1 - e^{(\theta_v - \theta_s)/C_1}. \quad (41)$$

The numerical solution of the two non-linear equations (39) and (41) gives the numerical values of the constants C_1 and C_2 in the case of minimization of Gauss constraint with respect to the temporal part, while those values could be obtained from the spatial part by solving equations (40) and (41).

The wetting front moisture content θ_v may be taken arbitrarily to be

$$\theta_v = \theta_1 + \alpha_v (\theta_s - \theta_1),$$

where α_v is a constant to be assumed.

NUMERICAL RESULTS

The technique just described has been applied to an alluvial sandy clay loam soil. The data used were taken from some experiments [5]. The initial water content θ_1 and the water content near the saturation θ_s were found to be 0.16 and 0.51 cm³/cm³ respectively. The soil water diffusivity $D(\theta)$ and the capillary conductivity $k(\theta)$ were fitted by the following exponential expressions:

$$D(\theta) = 64.865 \cdot 10^{-6} \exp(23.3858 \theta), \quad \text{for } \theta_1 \leq \theta \leq \theta_s, \quad (42)$$

$$k(\theta) = 64.549 \cdot 10^{-13} \exp(64.8697 \theta - 43.7416 \theta^2) \quad \text{for } \theta_1 \leq \theta \leq \theta_s. \quad (43)$$

The calculations are carried out to determine the water content distribution and the location of the wetting front and their variation with the time in the domain shown in Figure(1). The geometrical dimensions are $X = 55$ cm, $Z = 60$ cm and $R = 5$ cm. The constant α_v was assumed to be 0.15.

It should be noted that the minimization of Gauss constraint with

respect to the temporal complex yields much better results. Solution of the system of equations (39) and (41) by using Newton Raphson's method [7] gives the following results:

$$C_1 = 0.0782 \qquad C_2 = 0.9777$$

Substituting the above values into equations (21) , (26) , (27) and (28) and using the Romberg integration method [7] to evaluate the integral on the right-hand side of equation (28), we have:

$$\begin{aligned} B_1 &= 0.0915 & B_6 &= 0.2811 \\ B_7 &= 0.1147 & B_8 &= -0.0014 \end{aligned}$$

Substituting the numerical values of B_1 , B_6 , B_7 and B_8 in equations (33) and using the Runge-Kutta method [7] of integration we get the penetration depths q_1 and q_2 . The results are given in Table (1).

Table (1) Variation of the penetration depth with time for the irrigation by furrows for alluvial sandy clay loam soil

Time (min)	q_1 (cm)	q_2 (cm)
121	18.01	18.31
305	28.02	28.72
562	37.87	39.16
877	47.29	49.32

II. INFILTRATION FROM EQUALLY SPACED BURIED PIPES

The Gauss principle can also be applied to the case of infiltration from buried pipes. Figure (3) shows the buried pipes, which divide the region into symmetrical slabs. Each slab is subdivided into two parts, one of which lies above the x axis where the moisture content distribution takes the form

$$\theta = \theta_s + C_1 \ln \left(1 - C_2 \left(\frac{x^2}{q_1^2} + \frac{z^2}{q_3^2} \right) \right) \qquad (44)$$

and the other part lies below the x axis in which

$$\theta = \theta_s + C_1 \ln \left(1 - C_2 \left(\frac{x^2}{q_1^2} + \frac{z^2}{q_2^2} \right) \right), \qquad (45)$$

where $q_3(t)$, $q_1(t)$ and $q_2(t)$ are the penetration depths in the direction of negative z axis, positive x axis and positive z axis respectively.

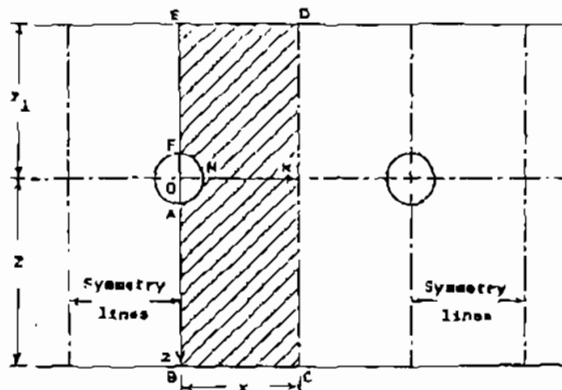


Fig. (3) Schematic diagram of a homogeneous soil irrigated by a set of circular buried pipes equally spaced at distances of $2X$.

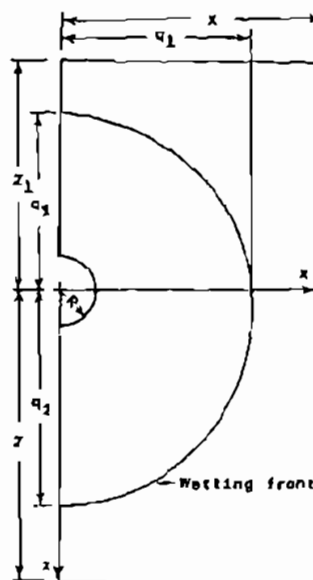


Fig. (4) Schematic diagram of the wetting front in the case of buried pipes.

The boundary conditions in this case are:

- 1 - $\theta = \theta_3$, $x = z = 0$; $t \geq 0$;
- 2 - $\frac{\partial \theta}{\partial x} = 0$; $x = 0$; $\left. \begin{array}{l} q_1 = q_2 = q_3 = R ; t = 0. \\ -q_3 < z < -R \\ R < z < q_2 \end{array} \right\}$.
- 3 - $\frac{\partial \theta}{\partial z} = 0$; $z = 0$; $R < x < q_1$.
- 4 - $\theta = \theta_w$ along the wetting front.

The analysis is analogous to that of the furrow case which leads to two systems of differential equations. The first system resulting from the minimization of the functional G with respect to the temporal complex \dot{q}_3/q_3 , \dot{q}_1/q_1 and \dot{q}_2/q_2 has the form:

$$\begin{aligned} \dot{q}_3 &= \frac{4B_6 - B_7}{8B_1} \frac{1}{q_3} - \frac{B_7}{8B_1} \frac{q_3}{q_1^2} + \frac{5B_8}{16B_1} , \\ \dot{q}_1 &= \frac{4B_6 - B_7}{8B_1} \frac{1}{q_1} - \frac{B_7}{8B_1} \frac{q_1}{q_3^2} + \frac{B_8}{16B_1} \frac{q_1}{q_3} , \\ \dot{q}_2 &= \frac{4B_6 - B_7}{8B_1} \frac{1}{q_2} - \frac{B_7}{8B_1} \frac{q_2}{q_1^2} - \frac{5B_8}{16B_1} , \end{aligned} \quad (46)$$

while the second system resulting from the minimization of the functional G with respect to the spatial complex $1/q_3^2$, $1/q_1^2$ and $1/q_2^2$ is :

$$\begin{aligned} \dot{q}_3 &= \frac{B_6(4B_2 - B_3 + B_4) - B_2 B_7}{B_6(2B_6 - B_7)} \frac{1}{q_3} - \frac{B_6(B_3 - B_4) - B_2 B_7}{B_6(2B_6 - B_7)} \frac{q_3}{q_1^2} \\ &+ \frac{1}{4} \frac{B_6(5B_9 - 2B_{10}) - B_7 B_9}{B_6(2B_6 - B_7)} + \frac{1}{4} \frac{B_5(3B_6 - B_7)}{B_6(2B_6 - B_7)} q_3, \\ \dot{q}_1 &= \frac{B_6(4B_2 - B_3 + B_4) - B_2 B_7}{B_6(2B_6 - B_7)} \frac{1}{q_1} - \frac{B_6(B_3 - B_4) - B_2 B_7}{B_6(2B_6 - B_7)} \frac{q_1}{q_3^2} \\ &+ \frac{1}{4} \frac{B_6(B_9 - 2B_{10}) + B_7 B_9}{B_6(2B_6 - B_7)} \frac{q_1}{q_3} - \frac{1}{4} \frac{B_5(B_6 - B_7)}{B_6(2B_6 - B_7)} q_1, \\ \dot{q}_2 &= \frac{B_5(4B_2 - B_3 + B_4) - B_2 B_7}{B_6(2B_6 - B_7)} \frac{1}{q_2} - \frac{B_6(B_3 - B_4) - B_2 B_7}{B_6(2B_6 - B_7)} \frac{q_2}{q_1^2} \\ &- \frac{1}{4} \frac{B_6(5B_9 - 2B_{10}) - B_7 B_9}{B_6(2B_6 - B_7)} + \frac{1}{4} \frac{B_5(3B_6 - B_7)}{B_6(2B_6 - B_7)} q_2. \end{aligned} \quad (47)$$

The values of B_1 to B_{10} in the last two systems are the same as stated before in equations (21) to (30).

The calculations were carried out for the same soil considered in the furrow case. So the constants C_1 , C_2 and B_1 to B_{10} have the same numerical values as before. The flow medium shown in Figure (3) has the following geometrical dimensions:

$$Z_1 = 40 \text{ cm}, \quad X = 45 \text{ cm}, \quad Z = 50 \text{ cm}, \quad R = 5 \text{ cm}.$$

The numerical solution of the system of equations (46) using Runge-Kutta method gives the penetration depths q_1 , q_2 and q_3 . The results are shown in Table (2).

Table (2) Variation of the penetration depth with time for the irrigation by buried pipes for alluvial sandy clay loam soil

Time (min)	q_3 (cm)	q_1 (cm)	q_2 (cm)
110	17.39	17.67	18.15
303	26.73	27.41	28.59
567	35.86	37.10	39.30

RESULTS AND DISCUSSIONS

The water content distribution after 877 minutes of infiltration by a furrow is designated by the iso-water content lines of 0.40, 0.45, 0.40, 0.30 and 0.21 cm^3/cm^3 , Figure (5).

Figure (6) shows the water content distribution after 567 minutes of infiltration from a buried pipe. The iso-water content lines are for values of 0.48, 0.45, 0.40, 0.30 and 0.21 cm^3/cm^3 .

It is clear from Figures (5) and (6) that the water content in the flow medium changes with time and space in both directions. The wetting front (lines of $\theta = 0.21$) advances outwards of the water source at a decreasing rate. The lines of equal water content close to the water source are wide apart compared with those close to the wetting front. The closeness of the equal water content lines indicates a steep gradient of θ . Klute (1) showed that the steep water content gradient at the wetting front is due to the strong dependence of $k(\theta)$ and hence $D(\theta)$ on the water content, Equations (42) and (43).

It is also noticed that for all considered times, the vertical penetration of water below the water source exceeds that in the horizontal direction for both cases of furrows and buried pipes. On the other hand in the case of buried pipes the penetration in the horizontal direction exceeds that in the vertical direction above the water source. This is due to the gravitational term $\partial k/\partial z$ in the flow Equation (1), (1).

Quantitative comparison between the results obtained by the Gauss technique and the ADI method (5) is discussed in view of the water content distribution in the x and z directions and the location of the wetting front. Figure (7) shows the water content distribution along x and z axes for the case of irrigation by open furrows while Figure (8) shows the water content distribution along negative z , x and positive z axes for the case of irrigation by buried pipes. The water content distribution was plotted as a function of the distance at two different time periods corresponding to two different infiltration depths for every single space coordinate, i.e. when the wetting front reaches a depth of 30 and 50 cm. below the centre of the furrow or 20 and 40 cm. below the centre of the pipe along the central vertical plane.

The location of the wetting front could serve as an index for comparing the calculated results using different methods. Figure (9) shows a comparison between the location of the computed wetting front using the ADI method and the Gauss technique as a function of time and space coordinates for the case of irrigation by open furrows. The same comparison for the case of irrigation by buried pipes is shown in Figure (10).

CONCLUSION

A comparison of water content distribution obtained by the ADI method and the Gauss technique is made for different periods of time along the horizontal and central vertical axes. The overall shape of the moisture distribution curves obtained by the Gauss technique and their dependence upon the infiltration time are in good agreement with

that computed using the ADI method. The most remarkable feature of the Gauss technique is that the computation time is reduced to about 1/900 of the time required to get the same results using the ADI method. Thus the Gauss technique is highly recommended whenever a trial function is available.

REFERENCES

1. Klute, A.: " A Numerical Method for Solving the Flow Equation for Water in Unsaturated Materials",
Soil Sci. Amer. Vol. 73, 1952, pp. 105 - 116.
2. Philip, J.R.: " The Theory of Infiltration 1 : The Infiltration Equation and its Solution ",
Soil Sci. Vol. 63, No. 5, 1957, pp. 345 - 357.
3. Philip, J.R.: " Absorption and Infiltration in Two- and Three-dimensional Systems",
Unesco Symposium on Water in the Unsaturated Zone, Vol. No. 1, 1966, pp. 503 - 525.
4. Selim, H.M. and Don Kirkham.: " Unsteady Two-Dimensional Flow of Water in Unsaturated Soils above an Impervious Barrier",
Soil Sci. Amer. Proc. 37, 1973, pp. 489 - 495.
5. Sollman, N.F., Bakr, H.M.A., Hassan, M.N. and Boutros, Y.Z.: "Unsteady Two-Dimensional Infiltration from Semi-Circular Furrow",
Journal of Soil Sciences, No. 29, 1978, pp. 22 - 31.
6. Vujanovic, B. and Baclic, B.: " Application of Gauss's Principle of Least Constraint to the Non-linear Heat Transfer Problems",
Int. J. Heat Mass Transfer. 37, 1975, pp. 721 - 730.
7. Bajpai, A.C., Calus, I.M. and Fairley, J.A.: "Numerical Methods for Engineers and Scientists",
John-Wiley and Sons Ltd, London, 1977.

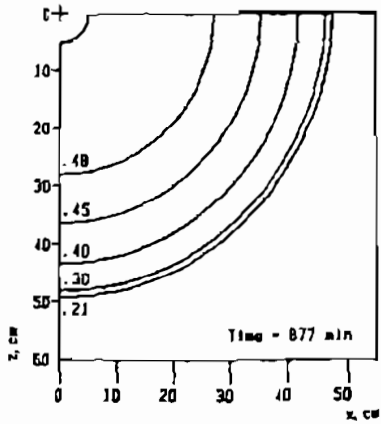


Fig.(5) Water content θ for irrigation by furrows.

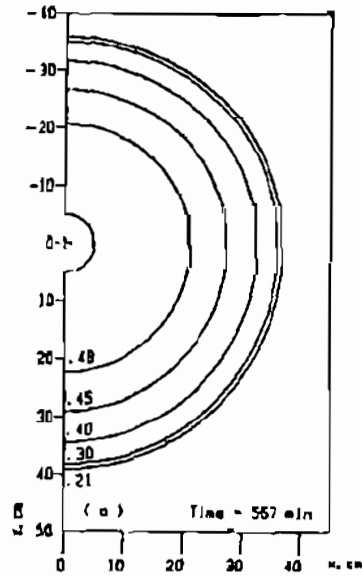


Fig.(6) Water content θ for irrigation by buried pipes.

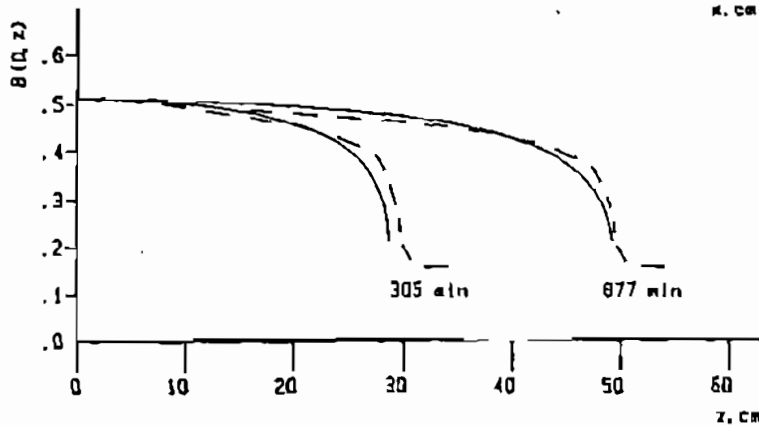
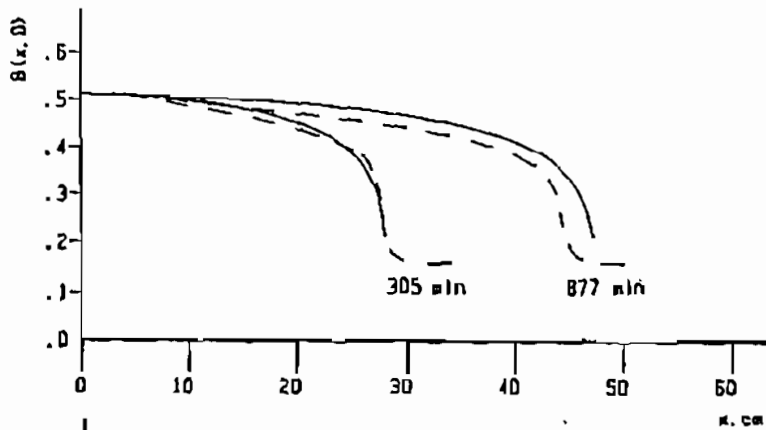


Fig.(7) Water content distribution $\theta(x, 0)$ and $\theta(0, z)$ as obtained by the Gauss principle technique (solid lines) and the ADI method (broken lines).

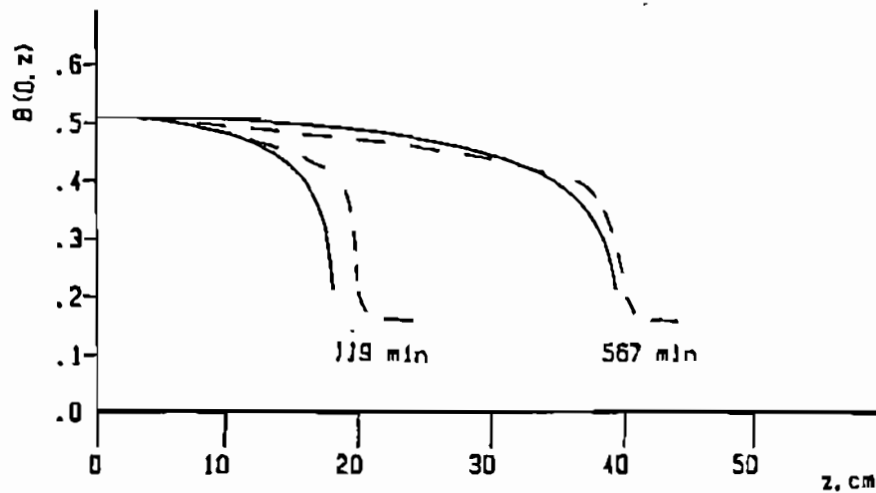
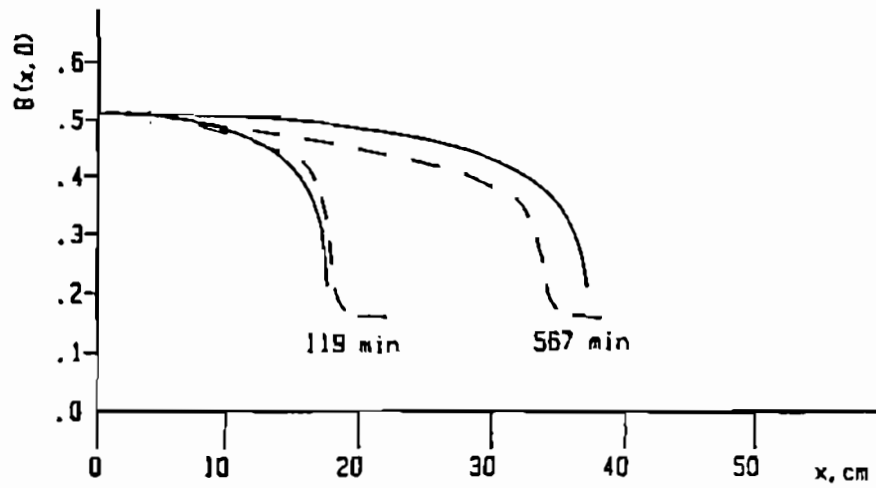
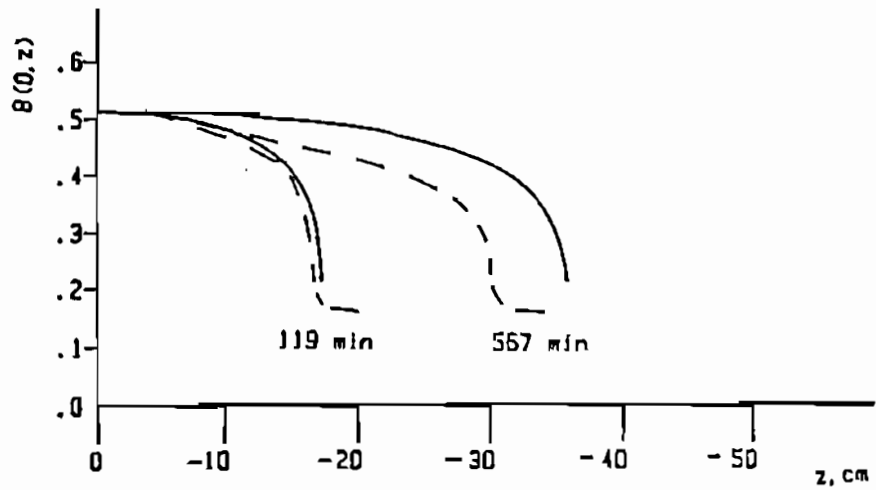


Fig.(8) Water content distribution $\theta(x, 0)$ and $\theta(0, z)$ as obtained by the Gauss principle technique (solid lines) and the ADI method (broken lines).

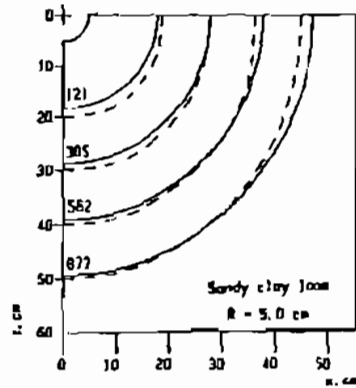


Fig.(9) Wetting front position for irrigation by open furrows as obtained by the Gauss technique (solid lines) and the ADI method (broken lines). Infiltration period in minutes is shown on the curves.

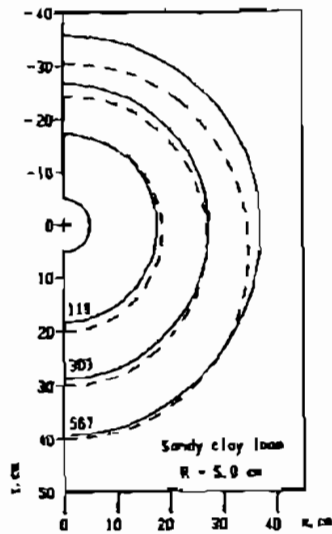


Fig.(10) Wetting front position for irrigation by buried pipes as obtained by the Gauss technique (solid lines) and the ADI method (broken lines). Infiltration period in minutes is shown on the curves.